Monatshefte für Chemie 128, 123–135 (1997)

Monatshefte für Chemie
Chemical Monthly

Mechanism and Kinetics of the Electrochemical Reduction of Cu(II) at Gold in Pyridine and Water-Pyridine Mixtures

M. Scendo and **J. Malyszko***

Institute of Chemistry, Pedagogical University, PL-25020 Kielce, Poland

Summary. The cathodic reduction of Cu(II) ions at a gold electrode has been studied in water-pyridine mixtures containing $NaClO_4$ as background electrolyte by means of rotating disc (RDE) and ring-disc electrode voltammetry (RRDE), coulometry, and potentiometry. The voltammetric curves obtained at the RDE split into two waves of nearly the same height which correspond to two successive reactions: $Cu(II) + e^- \rightarrow Cu(I)$ and $Cu(I) + e^- \rightarrow Cu$. The diffusion coefficients of Cu(II) as well as the formal potentials and kinetic parameters of the Cu(II)/Cu(I) electrode reaction were evaluated and are discussed. In addition, some experiments with an electrochemical quartz crystal microbalance (EQCM) were performed in order to explain the pyridine adsorption on polycrystalline gold.

Keywords. Copper; Electrochemical quartz crystal microbalance; Electrode kinetics; Mixed solvents; Pyridine; Rotating ring-disc electrode.

Mechanismus und Kinetik der elektrochemischen Reduktion von Cu(II)-Ionen an einer Goldelektrode in Wasser-Pyridin-Mischungen

Zusammenfassung. Die kathodische Reduktion von Cu(II)-Ionen an Gold in Wasser-Pyridin-Mischungen mit $NaClO_4$ als Grundelektrolyt wird mittels Voltammetrie an der rotierenden Scheiben- und Ring-Scheibenelektrode sowie mittels Coulometrie und Potentiometrie untersucht. Die erhaltenen Stromspannunskurven verteilen sich auf zwei Stufen, die den konsekutiven Durchtrittsreaktionen $Cu(II) + e^- \rightarrow Cu(I)$ und $Cu(I) + e^- \rightarrow Cu$ entsprechen. Die Diffusionskoeffizienten der Cu(II)-Ionen sowie die Formal-Standardpotentiale und die kinetischen Parameter der Cu(II)/Cu(I)-Durchtrittsreaktion wurden bestimmt und werden diskutiert. Zusätzliche Experimente zur Erklärung der Adsorption von Pyridin an polykristallinem Gold wurden mit Hilfe einer elektrochemischen Quarz-Mikrowaage durchgeführt.

Introduction

During the last years, considerable efforts have been made to understand the role of the solvent in the thermodynamics and kinetics of relatively simple charge transfer reactions at electrodes. In previous works [1–3] we have investigated the mechanism and kinetics of Cu(II) electroreduction in *DMSO* and *DMF* solutions and their mixtures with water. It was of great interest to extend these studies to pyridine

(*Py*), a solvent of great solvating power. The relative great value of the *Gutmann* donor number ($DN = 33.1$[4]) reflects its hard donor properties. Thus, pyridine is known to form relatively strong complexes with Cu(II) in aqueous solutions [5]. Beside its acceptor (nucleophilic) properties, *Py* is capable of soft–soft interactions with soft acceptors such as Cu(I), Ag(I), and Hg(II) [6]. The soft donor properties of solvents can be described by the *Gritzner* softness parameter [7], *SP*, based on the *Gibbs* energy of transfer of Ag(I) from benzonitrile to the respective solvent. It is worth noting that pyridine exhibitis also a large value of the softness parameter ($SP = 73$). In recent years, *Persson* and co-workers [8, 9] found that copper(I) is much more strongly solvated in pyridine than in water and that this increase is greater than for copper(II) ions. Consequently, Cu(I) ions are strongly stabilized wih respect to the disproportionation

$$2\mathrm{Cu(I)} \rightleftharpoons \mathrm{Cu(II)} + \mathrm{Cu} \tag{1}$$

The equilibrium constant of this reaction in *Py* was determined by the authors cited to $K_d = 1.1 \times 10^{-14}$.

To our knowledge, no kinetic and mechanistic data for the electrochemical Cu(II)–Cu(I)–Cu system in pyridine and pyridine-water media have been reported so far. The aim of this work is to examine the electrochemical reduction of Cu(II) on a polycrystalline Au electrode in the mentioned media and to elucidate the role of pyridine in this process. This electrode has been chosen because of the existence of data in the literature concerning the adsorption and orientation of *Py* molecules at the aqueous solution/gold interface [10, 11]. We intended also to determine the kinetic parameters for the Cu(II)/Cu(I) electrode reaction. For the detection and quantitative determination of the species Cu(I), rotating ring-disc electrode measurements (RRDE) were carried out. In addition, some experiments were performed with an electrochemical quartz crystal microbalance (EQCM). The EQCM is a simple and reliable *in situ* technique for measuring the surface concentration of species adsorbed at solid surfaces from solutions.

Results and Discussion

The cathodic reduction of $2 \times 10^{-3}\mathrm{mol} \cdot \mathrm{dm}^{-3}$ Cu(II) at the Au RDE was studied in pure pyridine and its mixtures with water. All solutions contained $0.4\,\mathrm{mol} \cdot \mathrm{dm}^{-3}$ $NaClO_4$ as a background electrolyte. The current *vs.* potential curves were recorded at different rotation frequencies of the RDE in the negative direction. A slow potential scan ($5\,\mathrm{mV} \cdot \mathrm{s}^{-1}$) was applied to minimize the contribution of adsorption/desorption kinetics in the currents recorded. Some typical voltammetric curves recorded at a rotation frequency of 30 Hz are depicted in Fig. 1. Similar curves were observed at other rotational velocities.

As expected, the reduction of Cu(II) occurs in two stages which may be attributed to two consecutive reactions according to the general scheme

$$\mathrm{Cu(II)} + \mathrm{e}^- \rightleftharpoons \mathrm{Cu(I)} \tag{2}$$

$$\mathrm{Cu(I)} + \mathrm{e}^- \rightleftharpoons \mathrm{Cu} \tag{3}$$

The first wave is well-separated from the second one. In a solution with $X_{Py} = 0.12$, one observes a minimum on the plateau of the first wave which gra-

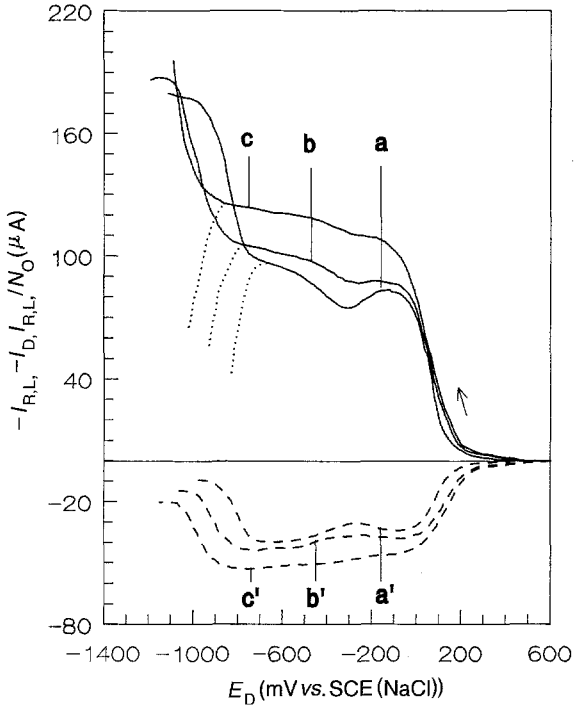

Fig. 1. Dependence of the disc current (solid lines), corresponding limiting ring current (dashed lines), and normalized limiting ring current (dotted lines) upon the disc electrode potential during the reduction of 2×10^{-3} mol · dm^{-3} Cu(II) at an Au electrode from solutions containing 0.4 mol · dm^{-3} $NaClO_4$ as a background electrolyte; mole fractions of *Py*: (a) 0.12, (b) 0.63, (c) 1.00; ring potential: 500 mV; rotation frequency: 30 Hz; potential scan rate: 5 mV · s^{-1}

dually disappears with increasing *Py* concentration. The nature of the plateau current for the one-electron reduction of Cu(II) was verified using the *Levich* equation. Except for the above mentioned *Py* concentration, plots of this current measured at a constant potential of the disc electrode were not quite linear, thus suggesting that the current is not convective diffusion controlled.

In order to explain the anomalies observed, experiments were performed employing RRDE voltammetry. In this series of experiments, the ring electrode potential was held on the current plateau for Cu(I) → Cu(II) oxidation. Next, the ring and the disc currents were followed as the disc electrode was scanned in the cathodic direction. Limiting ring current *vs.* disc potential curves for three solutions of various *Py* content are presented in the lower part of Fig. 1. The same Figure also shows the normalized ring current. As can be seen, the normalized limiting ring current parallels the disc current within the first wave for the reduction of Cu(II). Except for the solution with $x_{Py} = 0.12$, an increase in $I_{R,L}$ and thus in $I_{R,L}/N_0$ is observed in the bottom region of the second wave. At more negative potentials, the reduction of Cu(I) to metallic copper occurs and the ring current drops to zero as Cu(I) is consumed at the disc surface. This fact implies that (i) the limiting current of the first wave is not reached on its plateau and (ii) the electron-transfer reaction (2) still takes place in the potential range corresponding to the bottom of the second wave.

According to *Scheller* and co-workers [12, 13], the facts described above indicate that the electrode surface can be considered as a partially blocked one. The organic component of the solvent behaves as a typical surfactant-inhibitor over the whole concentration range studied. Consequently, the diffusion coefficients of Cu(II), $D_{Cu(II)}$, were determined basing on the maximal values of the ring current.

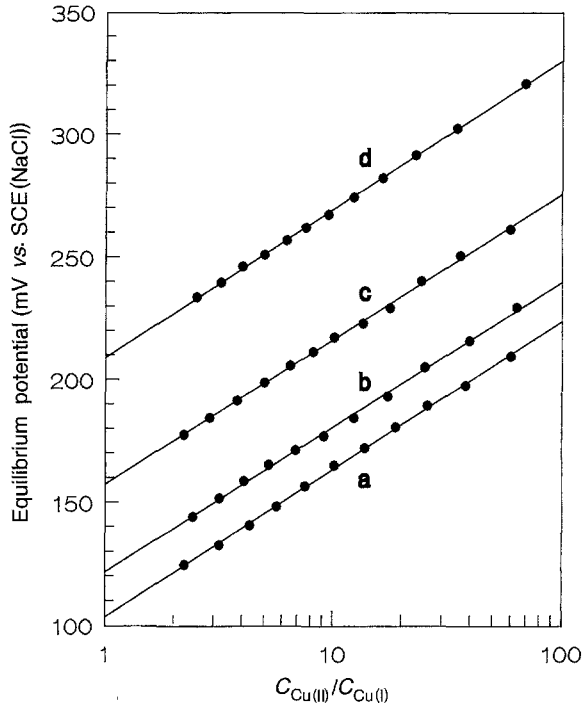

Fig. 2. Equilibrium electrode potentials of the Cu(II)/Cu(I) couple, referred to the aqueous SCE(NaCl), as a function of the concentration ratio in solutions containing 0.4 mol · dm^{-3} $NaClO_4$ as the background electrolyte; mole fractions of *Py*: (a) 0.12, (b) 0.25, (c) 0.46, (d) 1.00; initial Cu(II) concentration: 2× 10^{-3} mol · dm^{-3}

Table 1. Diffusion coefficients of Cu(II) ions, formal electrode potentials, formal rate constants, and cathodic transfer coefficients of the Cu(II)/Cu(I) system at an Au electrode in water r-pyridine mixtures; background electrolyte: 0.4 mol · dm^{-3} $NaClO_4$

x_{Py}	Viscosity ($10^2\eta$, cm^{-1} · g · s^{-1})	$10^6 D_{Cu(II)}$ (cm^2 · s^{-1})	E^0_{21} (mV *vs.* SCE(NaCl))	E^0_{21} (mV *vs. Fic*$^+$*/Foc*)	k_s (cm · s^1)	α_c
0	0.921	6.8	−135	−270	2.0×10^{-4}	0.37
0.12	2.046	1.2	104	−100	3.8×10^{-3}	0.50
0.25	1.929	1.0	122	−125	1.0×10^{-3}	0.49
0.36	1.823	1.0	142	−145	6.9×10^{-4}	0.48
0.46	1.735	1.1	158	−180	4.8×10^{-4}	0.47
0.63	1.585	1.4	200	−185	2.6×10^{-4}	0.45
0.76	1.473	1.6	205	−195	3.0×10^{-4}	0.43
1.00	1.255	1.9	209	−190	3.9×10^{-4}	0.42

The *Levich* plots were found to be satisfactorily linear and to pass through the origin. The obtained values of $D_{Cu(II)}$ are collected in Table 1.

In further experiments, the formal potentials of the Cu(II)/Cu(I) redox pair, $E^{0'}_{21}$, were determined using coulometric and potentiometric techniques as described earlier [1]. The $c_{Cu(II)}/c_{Cu(I)}$ ratio was changed by cathodic reduction of Cu(II) under coulometric control at constant current within the first wave. The total concentration of copper ions was maintained at 0.01 mol · dm^{-3}. Plots of the equilibrium potential against $\log c_{Cu(II)}/c_{Cu(I)}$ were linear (cf. Fig. 2). The slopes of 59 ± 3 mV/decade are in good agreement with the theoretical value for a one-electron redox reaction exhibiting the *Nernst* behaviour. The formal potentials were evaluated by extrapolation of these plots to $c_{Cu(II)}/c_{Cu(I)} = 1$.

In order to compare the formal potentials in various solvents, it is necessary to correct the experimental data for liquid junction potentials between the solvent used and the reference electrode. Hence, the values of E_{21}^0 were also expressed against the potential of the ferricinium ion/ferrocene (Fic^+/Foc) redox pair which was recommended by *Gritzner* and *Kuta* [14] as a solvent independent electrode. The formal potentials of the Fic^+/Foc electrode were evaluated from RDE voltammetric measurements under conditions identical to those used in the study of the Cu(II)/Cu(I) system.

The rate constants of the electron transfer reaction Cu(II)/Cu(I) in pyridine and *Py*-water mixtures were determined by means of the RDE technique, in a manner similar to that used in polarography for quasi-reversible waves by applying the relation given in Ref. [15]. For the evaluation of the kinetic parameters in pure aqueous solution, a modified version of the method of *Jahn* and *Vielstich* [16] was used [17, 18].

The potential dependencies of the rate constants (in a logarithmic scale) are presented in Fig. 3. Extrapolation of the graphs obtained to the formal potentials of the Cu(II)/Cu(I) couple furnished the standard (formal) rate constants k_s. The transfer coefficients a_c were calculated from the slopes of the appropriate lines. The kinetic parameters of the Cu(II)/Cu(I) electrode reaction are collected in Table 1 together with the corresponding values of E_{21}^0. As can be seen, a_c varies between 0.37 and 0.50. In addition, the kinetic parameters for electrode reaction in pure pyridine were determined at a Pt electrode to be $k_s = 4.0 \times 10^{-4}\text{cm} \cdot \text{s}^{-1}$ and $a_c = 0.25$.

Further, we have performed a semi-logarithmic analysis of the second wave by applying equations (4) and (5).

$$E = E_{10}^{0'} - \frac{RT}{F} \ln \chi_{OX} + \frac{RT}{F} \ln (I_{D,L} - I_D) \tag{4}$$

$$\chi_{OX} = 0.62 FAv^{-1/6} D_{OX} \omega^{1/2} \tag{5}$$

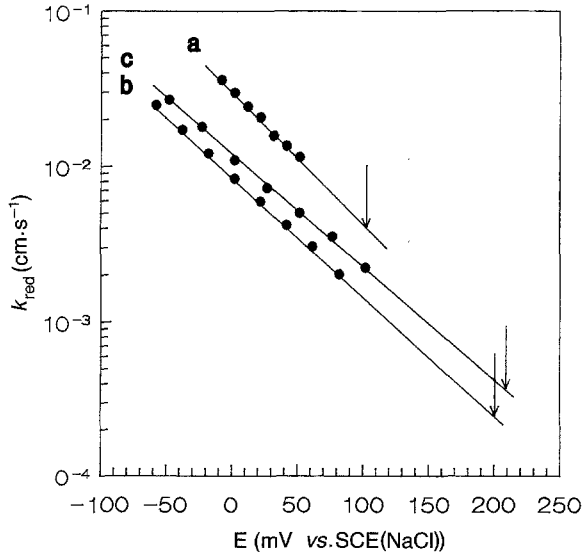

Fig. 3. Potential dependence of the cathodic rate constant k_{red} for the Cu(II)/Cu(I) electrode reaction in solutions containing 0.4 mol · dm^{-3} $NaClO_4$; mole fractions of *Py*: (a) 0.12, (b) 0.63, (c) 1.00; vertical bars indicate formal potentials

Here $E_{10}^{0'}$ is the formal potential of the Cu(I)/Cu redox system, I_D is the disc current within the second wave, $I_{D,L}$ is the limiting current of this wave, A is the geometric area of the disc, D_{OX} is the diffusion coefficient of the oxidized form of the reactant, and ν and ω denote the kinematic viscosity and the angular velocity of the electrode, respectively. The symbols R, T and F have their usual meaning. For the reversible half-wave potential, one obtains

$$E_{1/2r} = E_{10}^{0'} + \frac{RT}{F} \ln \frac{c_{OX}}{2} \tag{6}$$

where c_{OX} is the bulk concentration of the oxidized form of the reactant. The above expressions are valid for a reversible process with formation of an insoluble product which covers the whole electrode surface. They are similar those derived by *Meites* [19] for an analogous process occuring under polarographic conditions. It should be stressed that the knowledge of the formal potentials $E_{21}^{0'}$ and $E_{10}^{0'}$ allows the calculation of the equilibrium constant K_d for the disproportionation reaction (1).

Figure 4 presents the semi-logarithmic analysis of the second wave for solutions of X_{Py} from 0.12 to 0.63. At pyridine contents above 0.63, the limiting current plateau of the second wave was not attainable because of decomposition of the background electrolyte at more positive potentials. The analysis was performed in a normalized form by dividing the difference $I_{D,L} - I_D$ by the limiting current of the second wave, $I_{D,L}$. The plots obtained are linear only at the upper part of the waves. The reciprocal slopes of these portions of the plots are 120, 94, 65, and 77 mV/decade for mole fractions of *Py* equal to 0.12, 0.25, 0.46, and 0.63, respectively. These values are too large to describe the waves as reversible because the theoretically expected value for a reversible one-electron process is 59 mV/decade. Consequently, the determination of values for K_d was not possible from the voltammetric data.

Further investigations towards a better understanding of pyridine adsorption at gold were performed using the electrochemical quartz crystal microbalance tech-

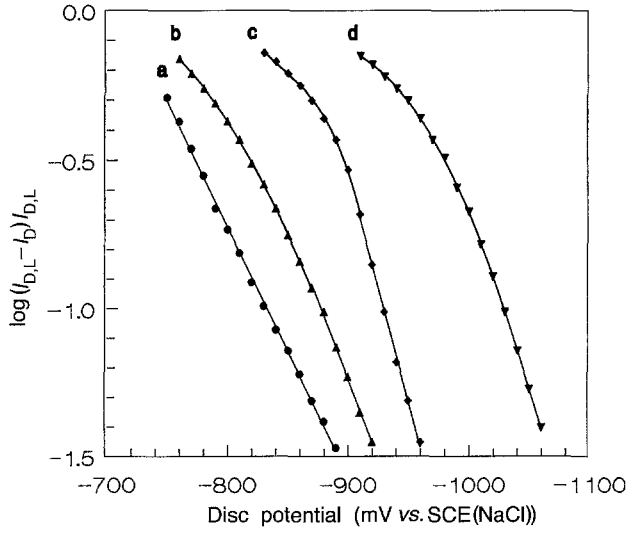

Fig. 4. Semi-logarithmic analysis of the second wave of Cu(II) at an RDE in solutions containing 2×10^{-3} mol · dm^{-3} $Cu(ClO_4)_2$ and 0.4 mol · dm^{-3} $NaClO_4$; mole fractions of *Py*; (a) 0.12, (b) 0.25, (c) 0.46, (d) 0.63; rotation frequency: 10 Hz; potential scan rate: 5 mV · s^{-1}

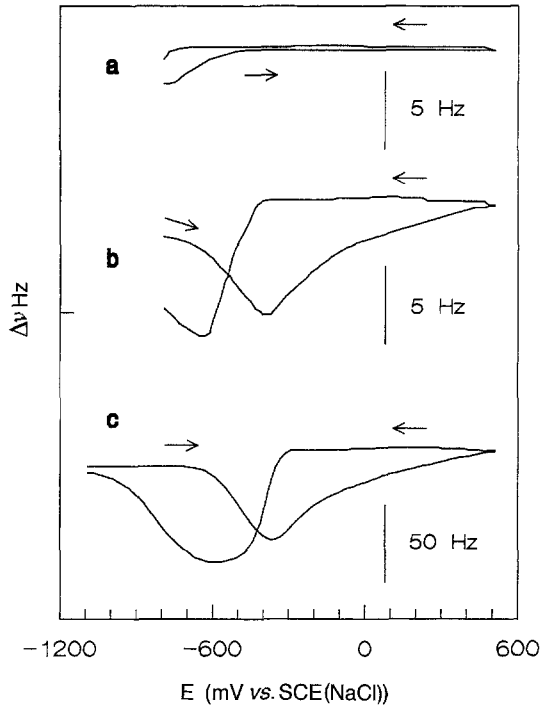

Fig. 5. Frequency change *vs.* potential curves of an Au-EQCM electrode in an aqueous solution containing $0.4\,\text{mol}\cdot\text{dm}^{-3}$ $NaClO_4$ during a single cycling scan originating from -0.8 V; sweep rate: $5\,\text{mV}\cdot\text{s}^{-1}$; (a) residual, (b) 1×10^{-3}, (c) $5\times10^{-2}\,\text{mol}\cdot\text{dm}^{-3}$ *Py*

nique (EQCM). In this technique, the change in resonant frequency Δf caused by a species rigidly adsorbed on the surface is a function of change in mass (Δm) of the quartz crystal as indicated by Eq. (7) [20].

$$\Delta f = -k_f \Delta m/A \tag{7}$$

In this relationship, k_f is the mass sensivity and A is area of the quartz plate undergoing oscillation between the two electrodes on opposite faces.

Figure 5 shows frequency change *vs.* potential curves obtained in $0.4\,\text{mol}\cdot\text{dm}^{-3}$ $NaClO_4$ solution in the absence (curve a) and presence of 1×10^{-3} and $5\times10^{-2}\,\text{mol}\cdot\text{dm}^{-3}$ pyridine (curves b and c, respectively). The residual Δf *vs.* E response curve shows little change during the positive and following negative scan (between -0.8 and 0.5 V). After the potential scan, the mass change returns to zero.

For the presence of $1\times10^{-3}\text{mol}\cdot\text{dm}^{-3}$ *Py* (curve b), a rapid decrease in frequency (*i.e.* mass increase) is observed during the initial portion of the positive scan and reaches a broad minimum in the potential range between -0.6 and -0.1 V as a result of the adsorption of pyridine. It should be stressed that the electrode was initially held at $E = -0.8$ V in order to desorb *Py* molecules from its surface. With continued positive scan, a gradual frequency increase (*i.e.* mass decrease) occurs in the range up to 0.5 V. During the backward scan from 0.5 to 0.25 V, the frequency continues to rise, but its change is not large. A further potential change in the negative direction results in a Δf *vs.* E curve similar to that obtained during the positive scan but shifted towards negative potentials. Of great significance is the fact that the frequency observed at the termination of the cyclic scan does not equal the frequency at the start of the scan ($\Delta f = -3.8\,\text{Hz}$, $\Delta m/A =$

$7.5 \times 10^{-8}\,g \cdot cm^{-2}$). The above facts point to a slow desorption of pyridine from the gold surface. About 3 min after each terminated run were required to achieve the initial frequency at a potential of −0.8 V.

In the case of a 5×10^{-2} mol · dm^{-3} *Py* solution, the frequency shift is roughly ten times greater than that observed in the previous solution. Under these conditions, the composition of the surface phase becomes similar to that of the bulk of solution. As a consequence, the thickness of the liquid layer attached to the electrode surface increases and thus changes drastically the coupling between electrode and solution. A similar phenomenon was reported by *Stökel* and *Schumacher* [21] in the case of hydrogen chemisorption at a Pt electrode from aqueous solutions of sulfuric acid.

As can be seen from Table 1, the diffusion coefficient of Cu(II), $D_{Cu(II)}$, decreases as the mole fraction of *Py* rises to a value of approximately 0.3. With further increasing *Py* content in the solution, a gradual increase of $D_{Cu(II)}$ is observed. This behaviour is mainly due to the changes in viscosity of the solution (η, also reported in Table 1). On the other hand, the diffusion coefficient is also a function of the changes in solvent structure and solvation of Cu(II). The latter effects can be analyzed from the variation of the *Walden* product, $D_{Cu(II)}\,\eta$, with the solvent composition to avoid the effect of bulk viscosity. The variation of $D_{Cu(II)}\,\eta$ with x_{Py} is shown in Fig. 6 (curve b). A significant decrease of the *Walden* product with respect to that of pure water can be observed up to about $x_{Py} = 0.4$. Since the product discussed is inversely proportional to the solvated radius of the ion, according to the *Stokes-Einstein* relation the decrease in $D_{Cu(II)}\,\eta$ points to an increase of the Cu(II) radius due to the progressive substitution of water molecules by more voluminous pyridine ones in the coordination shell. At x_{Py} values close to 0.4, the *Walden* product passes through a broad maximum and thereafter becomes a slightly increasing quantity. This effect cannot be explained simply by a change in the *Stokes* radius of Cu(II). Although the exact mechanism is not clear at present, one of the origins might be ascribed to changes in the solvent structure.

The kinetics of electrochemical reactions in aqueous-organic solvent mixtures depend on the solvation properties of the reactants in the bulk of solution as well as on the adsorption of the organic solvent which modifies the structure of double layer at the electrode surface. Systematic studies of the adsorption of pyridine at

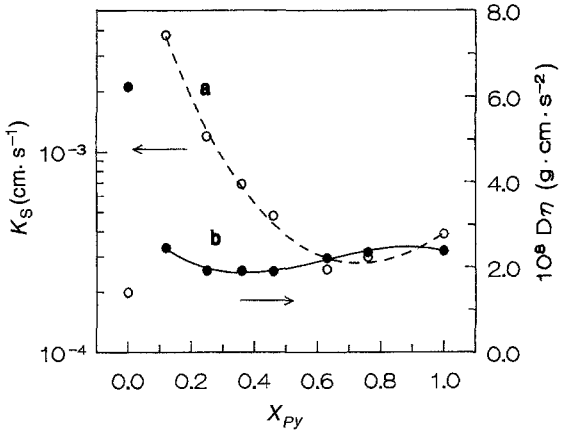

Fig. 6. Dependence of the standard (formal) rate constant for the Cu(II)/Cu(I) system (curve a) and the *Walden* product for Cu(II) (curve b) on the mole fraction of *Py*

polycrystalline Au and oriented single crystal surfaces of gold from aqueous solutions were performed by *Lipkowski* and co-workers using chronocoulometry ([22–25]; for reviews, see Refs. [9, 10]). The authors stated that the adsorption of pyridine at gold shows a strong dependence on the surface crystallography. At densely packed surfaces such as Au(111) and Au(100), two-state adsorption was observed. The pyridine molecules adopt a flat π-bonded orientation at the negatively charged surface and a vertical N-bonded position at the positive charged surface. On the contrary, at the "open" surfaces pyridine adopts only the vertical N-bonded orientation over the whole potential range. Consequently, pyridine molecules are non-uniformly distributed at the polycrystalline surface. The complete desorption of pyridine from a polycrystalline Au surface occurs in the potential range from -0.5 to -0.6V *vs.* SCE [10, 11].

Wieckowski and co-workers [26, 27] have investigated the pyridine adsorption at a polycrystalline gold electrode using radiochemical measurements. The dependencies of the surface concentration of *Py* on the electrode potential obtained agree quite well with those based on chronocoulometric measurements except for the positive potential range (*i.e.* beyond the "double layer region").

Comparing our results obtained for a 1×10^{-3} mol $\cdot$ dm^{-3} *Py* solution using the EQCM technique with the radiochemical data reported by *Wieckowski* and co-workers results in a good qualitative agreement. The maximum value of $\Delta m/A$ obtained by us corresponds to the surface concentration of pyridine Γ_{Py} equal to 7.4×10^{-10} mol $\cdot$ cm^{-2}, assuming a surface roughness of 1.7. This value is close to that reported by *Wieckowski* (about 6.5×10^{-10} mol $\cdot$ cm^{-2}). The frequency shift observed in the solution containing 5×10^{-2} mol $\cdot$ dm^{-3} *Py* is much larger than the changes caused by pyridine adsorption/desorption at gold.

Adsorption of pyridine from aqueous solutions at a Pt(111) electrode surface has been studied by *Hubbard* and co-workers [28]. The adsorbed molecules were found to have a nearly vertical orientation with a tilt angle of about 72°. It is interesting that in this case the packing density does not vary appreciably with electrode potential and adsorbate concentration.

The kinetics of the Cu(II)/Cu(I) electrode reaction should above all be considered in the terms of adsorption and orientation of the pyridine molecules at the gold/solution interface. It seems that these processes modify to a great extent the reaction which occurs in the higher potential range. It should be noted that position of the minimum on the RDE voltammogram (Fig. 1, curve a) coincides well with the maximum of *Py* adsorption at a polycrystalline gold electrode. From the facts presented above it can be concluded that reaction (1) proceeds in water-pyridine mixtures at a gold surface occupied by vertically oriented *Py* molecules.

As can be seen from Fig. 6, the standard (formal) rate constant in a solution of $x_{Py} = 0.12$ is about 20 times higher than that in a pure aqueous solution. This fact may be interpreted considering the solvation of the gold electrode surface and the reacting ion, Cu(II). At $x_{Py} = 0.12$, the electrode surface layer is preferentially solvated by pyridine, whereas Cu(II) ions remain partially hydrated. Since pyridine molecules are adsorbed more strongly than those of water, the surface concentration of the activated complex will be higher in their presence than in pure aqueous solution. In consequence, the reaction rate should also be higher.

On the other hand, the presence of a more basic solvent in the coordination sphere of the reactant increases the activation energy of its electrode reaction due to stronger interactions between the reactant ions and organic solvent molecules [29–31]. Obviously, both mentioned effects may partially compensate. Thus, the further decrease in k_s observed at $x_{Py} > 0.12$, where Cu(II) is mostly solvated by pyridine molecules, must be interpreted in these terms.

It should be stressed that the observed cathodic transfer coefficient a_c does not change substantially upon the gradual increase of *Py* concentration. This fact indicates that the transition state remains at nearly the same distance from the electrode surface in the whole composition range of the mixture.

In addition, we have listed literature data for the equilibrium constant of Cu(I) as well as for the kinetics of the Cu(II)/Cu(I) electrode reaction at platinum and gold electrodes in various solvents (Table 2). On the basis of the data presented in this Table, it can readily be seen that the apparent transfer coefficient, a_c, is generally close to 0.5 (except for a Pt electrode in *Py*), the value predicted by the theory of *Dogonadze* [32] for simple heterogeneous electron-transfer reactions. Moreover, the changes in the standard rate constant are not very large when going from one solvent to another.

In order to check if the dielectric relaxation behaviour of the solvent plays a role in the kinetics of reaction (1), we have analyzed the data for Pt electrodes on the basis of the theory given by *Fawcett* and co-workers [33–35]. According to their considerations, the formal rate of the electrode reaction can be expressed as follows:

$$\ln k_s = \ln k_0 - \kappa \ln \tau_L - g\gamma \tag{8}$$

(k_0: solvent-independent value of the standard rate constant, κ: degree of reaction adiabacity (a fraction between 0 and 1), τ_L: longitudinal relaxation time, γ: polarity parameter of the solvent (*Pekar* factor). According to the *Marcus* theory, g is a collection of some constants divided by the effective radius of the reactant. The polarity parameter of the solvent is defined as the difference of the optical

Table 2. Comparison of the equilibrium constant K_d for disproportionation reaction (1) and the kinetic parameters for Cu(II)/Cu(I) couple in various media as taken from the literature and the present work; the table also contains values of some parameters for the solvents considered

	DN	*SP*	γ	τ_L (ps)	K_d	Electrode	k_s (cm · s^{-1})	a_c
Water	21.9		0.127	0.85	1.3×10^{6}[a]	Pt	8.8×10^{-4}	0.49[b]
						Au	2.6×10^{-4}	0.38[c]
AN	14.1	32	0.466	0.19	8.3×10^{-20}[d]	Pt	3.5×10^{-3}	0.55[e]
DMF	26.6		0.311	1.6	1.8×10^{4}[f]	Pt	4.2×10^{-3}	0.52[f]
DMSO	29.8		0.188	3.2	1.9×10^{0}[g]	Pt	1.8×10^{-4}	0.44[b]
Py	33.1	73	0.359	1.3	1.1×10^{-14}[h]	Pt	4.0×10^{-4}	0.25[i]
						Au	3.9×10^{-4}	0.42[i]

[a] Ref. [39], [b] Ref. [2], [c] Ref. [40], [d] Ref. [41], [e] Ref. [42], [f] Ref. [3], [g] Ref. [1], [h] Ref. [8], [i] this work; data concerning the dielectric relaxation for electrolyte solutions in various solvents were taken from works of *Barthel* and co-workers; [43] (water), [44] (*AN*), [45] (*DMF*), [46] (*DMSO*)

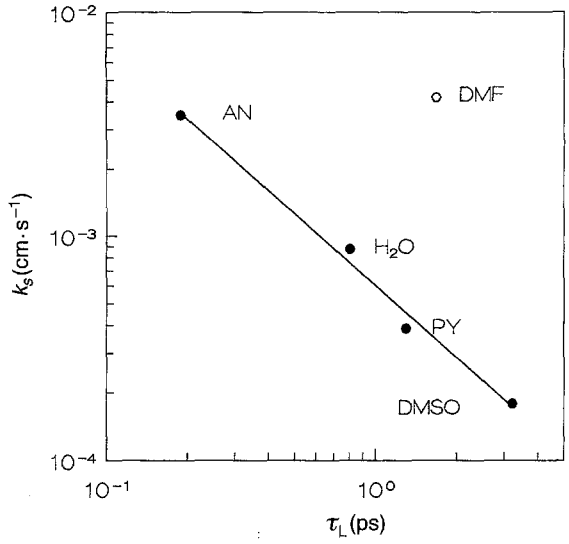

Fig. 7. Formal rate constants for the Cu(II)/Cu(I) electrode reaction on platinum plotted against the longitudinal relaxation time of the solvent using logarithmic scales

dielectric constant, ε_∞, and that of the static dielectric constant, ε_s:

$$\gamma = 1/\varepsilon_\infty - 1/\varepsilon_s \tag{9}$$

The standard rate constant of the Cu(II)/Cu(I) reaction on platinum is plotted against τ_L on logarithmic scales in Fig. 7. A good linear relationship with a slope equal to -1.07 is obtained for four solvents, *i.e. AN*, water *Py*, and *DMSO*. In this case, the correlation between $\log k_s$ and $\log \tau_L$ is strong ($r = 0.993$). One can assume (within experimental error) that κ is equal to 1; thus, the effects of the solvation dynamics predominate in the pre-exponential factor of the rate constant, and the reaction is adiabatic in these solvents. On the other hand, the correlation between $\ln k_s$ and γ in the solvents considered is very weak; therefore, the analysis is not completely reliable.

Experimental

Pyridine (Fluka, puriss., absolute) was used as obtained. Water used in these experiments was triply distilled. As a source of Cu(II) ions, copper(II) perchlorate hexahydrate and anhydrous copper(II) acetate were used. $Cu(ClO_4)_2 \cdot 6H_2O$ was obtained from the corresponding basic carbonate (POCh, p.a.) by neutralization with 60% $HClO_4$ (Merck, p.a.). Cupric acetate (POCh, p.a.) and sodium perchlorate (Merck, p.a.) were purified by two recrystallizations from water. The salts were dried at 110 and 140°C, respectively, for two days before use. Ferricinium picrate was prepared according to *Kolthoff* and *Thomas* [36].

Before the beginning of each electrochemical experiment, the solution was de-aerated by passing pure argon presaturated with the solution studied through the solvent.

The RRDE used in this study was constructed in our laboratory. Both disc and ring were made from gold of high purity (99.99% Au). The RRDE had the following parameters: $r_1 = 0.250$, $r_2 = 0.274$, $r_3 = 0.374$ cm. The geometric area of the disc was $A = 0.196\,\text{cm}^2$. The collection efficiency N_0 was determined experimentally with the Cu(II)/Cu(I) redox couple in chloride medium to be 0.42 ± 0.01. Some voltammetric experiments were also performed using a Pt RDE with the same geometric area. Another Au RDE with a geometric area of $0.521\,\text{cm}^2$ was applied as the generating electrode in coulometry. The working electrodes were polished by hand using alumina powders of

different grain sizes down to 0.05 μm on a microcloth wetted with water to achieve a mirror finish. Subsequently, the polished electrodes were sonicated carefully in water to remove impurities, and then rinsed successively with water and acetone.

A three-compartment electrochemical cell was used to separate working, reference, and counter electrode. Electrode potentials were measured and quoted with respect to an external saturated calomel electrode with NaCl solution (SCE(NaCl)). The counter electrode was a spiral-shaped Pt wire.

The electrochemical setup for voltammetric measurements consisted of an bipotentiostat Model 10/0.2 (University of Lodz) modulated by a linear programmer (University of Lodz) and coupled to a Model 4103 X – Y recorder (Laboratorni Pristroje). Ring-disc voltammograms were obtained utilizing a Model TZ 4200 dual pen Y – Y′ – t recorder (Laboratorni Pristroje).

Coulometric measurements were carried out with an OH-404 coulometer (Radelkis). Potentials were measured using a Model V-540 digital voltmeter (Meratronik).

The EQCM apparatus was constructed at the Institute of Physical Chemistry (Warsaw) according to a published design [37]. Planar At-cut quartz crystals (Phelps Electronics) of 1.4 cm in diameter were operated at a fundamental frequency of 5 MHz. Gold film electrodes (0.323 cm^2 area) were evaporated onto the crystals. The roughness factor of the electrode surface was determined measuring the quantity of charge required to form a layer of adsorbed oxygen [38] and was found to be 1.7. The value of k_f for our EQCM was determined experimentally from df/dQ for silver electrodeposition/dissolution [37] to be 5.05×10^7 Hz · cm^2 · g^{-1}. The changes in resonance frequency of the quartz oscillator due to mass change were measured on a Philips PM 6685 frequency counter and recorded on a Model 4103 X – Y recorder. The frequency resolution of the measurement was approximately 0.2 Hz.

Other details concerning the apparatus, the electrochemical cells, and the pretreatment of the electrodes are given in previous papers [2, 3].

All electrochemical experiments were carried out at 25 ± 0.2°C. The densities of the solutions were measured picnometrically. The viscosities were determined using an *Ubbelohde* viscometer.

Acknowledgements

This work was supported in part by the *State Committee for Scientific Research* (*KBN*) under Grant No. 1217/P3/92/02 (20007 91 01). The authors thank Mrs. *M. Kaczor* for technical assistance in some of the experiments.

References

[1] Malyszko J, Scendo M (1987) Monatsh Chem **118**: 435
[2] Malyszko J, Scendo M (1988) J Electroanal Chem **250**: 61
[3] Malyszko J, Scendo M (1989) J Electroanal Chem **269**: 113
[4] Gutmann V (1978) The Donor-Acceptor Approach to Molecular Interactions. Plenum Press, New York, p 20
[5] Inczedy J (1976) Analytical Applications of Complex Equilibria. Akademiai Kiado, Budapest, chapter 4
[6] Gritzner G, Sperker S (1990) J Solut Chem **19**: 543
[7] Gritzner G (1989) Z Phys Chem NF **156**: 99
[8] Ahrland S, Ishiguro S, Persson I (1986) Acta Chem Scand **A40**: 418
[9] Persson I (1986) Pure Appl Chem **58**: 1153
[10] Lipkowski J, Stolberg L (1992) Molecular Adsorption at Gold and Silver Electrodes. In: Lipkowski J, Ross PN (eds) Adsorption of Molecules at Metal Electrodes. VCH, Weinheim, p 171

[11] Lipkowski J, Stolberg L, Yang D-F, Pettinger B, Mirwald S, Henglein F, Kolb DM (1994) Electrochim Acta **39**: 1045
[12] Scheller F, Landsberg R, Wolf H (1970) Electrochim Acta **15**: 525
[13] Scheller F, Landsberg R, Wolf H (1970) Z Phys Chem **243**: 345
[14] Gritzner G, Kuta J (1984) Electrochim Acta **29**: 869
[15] Malyszko J (1975) Chimia **29**: 166
[16] Jahn D, Vielstich W (1962) J Electrochem Soc **109**: 849
[17] Malyszko J, Gierulska D (1984) Monatsh Chem **115**: 1401
[18] Malyszko J, Scendo M (1989) J Electroanal Chem **269**: 113
[19] Meites L (1965) Polarographic Techniques. Interscience, New York, chapter 4
[20] Sauerbrey G (1969) Z Phys **155**: 206
[21] Stöckel W, Schumacher R (1987) Ber Bunsenges Phys Chem **91**: 345
[22] Stolberg L, Richer J, Lipkowski J, Irish DE (1986) J Electroanal Chem **207**: 213
[23] Stolberg L, Lipkowski J, Irish DE (1987) J Electroanal Chem **238**: 333
[24] Stolberg L, Lipkowski J, Irish DE (1990) J Electroanal Chem **296**: 171
[25] Stolberg I, Lipkowski J, Irish DE (1991) J Electroanal Chem **300**: 563
[26] Lipkowski J, Stolberg L, Morin S, Irish DE, Zelenay P, Gamboa M, Wieckowski A (1993) J Electroanal Chem **355**: 147
[27] Zelenay P, Rice-Jackson LM, Wieckowski A (1990) Langmuir **6**: 974
[28] Stern DA, Laguren-Davidson L, Frank DG, Gui JY, Chiu-Hsun Lin, Lu F, Salaita GN, Walton N, Zapien DC, Hubbard AT (1989) J Am Chem Soc **111**: 877
[29] Broda J, Galus Z (1986) J Electroanal Chem **198**: 233
[30] Maksymiuk K, Galus Z (1987) J Electroanal Chem **234**: 361
[31] Maksymiuk K (1993) Electrochim Acta **38**: 721
[32] Dogonadze RR (1971) Theory of Molecular Electrode Kinetics. In: Hush NS (ed) Reactions of Molecules at Electrodes. Wiley, New York, p 135
[33] Fawcett WR, Foss CA (1991) Electrochim Acta **36**: 1767
[34] Fawcett WR, Fedurco M (1993) J Phys Chem **97**: 7075
[35] Fawcett WR, Opallo M (1994) Angew Chem Int Ed Engl **33**: 2131
[36] Kolthoff IM, Thomas FG (1968) J Phys Chem **69**: 3049
[37] Koh W, Kutner W, Jones MT, Kadish KM (1993) Electroanalysis **5**: 209
[38] Woods R (1976) Chemisorption at Electrodes. In: Bard AJ (ed) Electroanalytical Chemistry, vol 9. Marcel Dekker, New York, p 1
[39] Malyszko J, Duda L (1975) Monatsh Chem **106**: 633
[40] Malyszko J, Stepnik-Swiatek B (1990) J Electroanal Chem **292**: 175
[41] Estebesov SA, Molodov AI, Kolotirkin YM (1981) Elektrokhimiya **17**: 1890
[42] Kowalski TA, Lingane PJ (1971) J Electroanal Chem **31**: 1
[43] Barthel J, Krüger J, Schollmeyer E (1977) Z Phys Chem NF **104**: 59
[44] Barthel J, Kleebauer M, Buchner R (1995) J Solut Chem **24**: 1
[45] Barthel J, Bachhuber K, Buchner R (1994) Z Naturforsch **50a**: 65
[46] Behret H, Schmithals F, Barthel J (1975) Z Phys Chem NF **96**: 73

Received January 25, 1996. Accepted (revised) September 30, 1996